Journal of Applied Polymer Science

Melt rheology and mechanical crystal transformation in an immiscible blend with poly(vinylidene fluoride) matrix

Tingmao Zhu, Ruihua Lv, Bin Wang, Bing Na, Ming Yin, Yun Zhu
Fundamental Science on Radioactive Geology and Exploration Technology Laboratory, School of Chemistry, Biology and Materials Science, East China University of Technology, Nanchang 330013, People's Republic of China
Correspondence to: B. Na (E-mail: bna@ecit.edu.cn or bingnash@163.com)

ABSTRACT: Effect of immiscible polyamide 6 (PA6) on the melt rheology and stretch-induced crystal transformation of poly (vinylidene fluoride) (PVDF) matrix is reported. PA6 is dispersed as submicron droplets in the PVDF matrix, responsible for significant enhancement in the melt elasticity. Nevertheless, crystallization habits of PVDF matrix from melt are little affected by submicron PA6 droplets, and the α-form of PVDF prevails in the blends. Upon mechanical stretching, the α-form is converted to the β-form, which is remarkably reduced with the increasing of PA6 content in the blends. It could be correlated with the decreased tensile stress in the presence of submicron PA6 droplets that act as stress concentrators. © 2016 Wiley Periodicals, Inc. J. Appl. Polym. Sci. **2016**, *133*, 43499.

KEYWORDS: blends; properties and characterization; rheology

Received 28 November 2015; accepted 30 January 2016
DOI: 10.1002/app.43499

INTRODUCTION

Poly (vinylidene fluoride) (PVDF) is a semicrystalline polymer with good chemical resistance and physical properties. However, it usually suffers from low ductility and toughness. To overcome this limitation, a common route is to blend PVDF with other polymers.[1–5] The miscibility is a key factor to affect structural formation and resulted properties of the blends. PVDF is immiscible with most polymers due to lack of enough chain interactions.[6–9] The second component is dispersed as micron droplets in the PVDF matrix, and there exists remarkable phase interface between two components. Thus, in the past, much attention was paid to tailor phase morphology and interfacial interactions in the blends by introducing compatibilizers.[10–15]

Polyamide 6 (PA6), an engineering plastics, is also immiscible with PVDF over the whole composition range.[16–19] However, due to the presence of specific interactions between two components,[17,18] submicron PA6 droplets can be generated in the PVDF matrix under normal processing conditions. It is responsible for enhanced ductility and toughness of PVDF/PA6 blends. On the other hand, crystallization habit of PVDF matrix is little affected by PA6 droplets; and the α-form is usually produced for PVDF matrix upon cooling from melt.

Understanding of rheological properties is critical to optimize processing conditions for PVDF/PA6 blends. Rheological properties are very sensitive to blend morphology in the melt. While submicron droplet morphology is taken into account, it is expected that rheological properties of the PVDF matrix could be significantly affected by adding PA6. On the other hand, stretching of PVDF can induce transformation of the α-form into the β-form, which has been well demonstrated.[20–22] Formation of the β-form that is electrically active is of great interest for the extended applications of PVDF. As illustrated above, blending of PVDF with PA6 is beneficial for the improvement in the mechanical properties. However, effect of PA6 droplets on the crystal transformation of PVDF matrix is absent yet.

The results in this study clearly demonstrate that the presence of PA6 droplets remarkably enhances melt elasticity and viscosity of PVDF matrix. It arises from large interfacial area and good interfacial interactions in the blends. On the other hand, α→β crystal transformation in the PVDF matrix is suppressed, which becomes severe with the increasing of PA6 content in the blends.

EXPERIMENTAL

Materials and Sample Preparation

The PVDF (tradename FR907) was provided by shanghai 3F new materials Co. Ltd, China and had a melt flow index of 8 g/10 min (230 °C, 2.16 kg). The PA6 (tradename YH3400), with a relative viscosity of 3.3, was purchased from Baling petroleum and chemical corporation of China. Prior to blending, both materials were vacuum dried at 80 °C for 24 h. Melt blending of PVDF with PA6 was carried out in a twin-screw extruder at 240 °C with a screw speed of 15 rpm. The PA6 content in the blends was 15 and 30 wt % (by weight), respectively. For

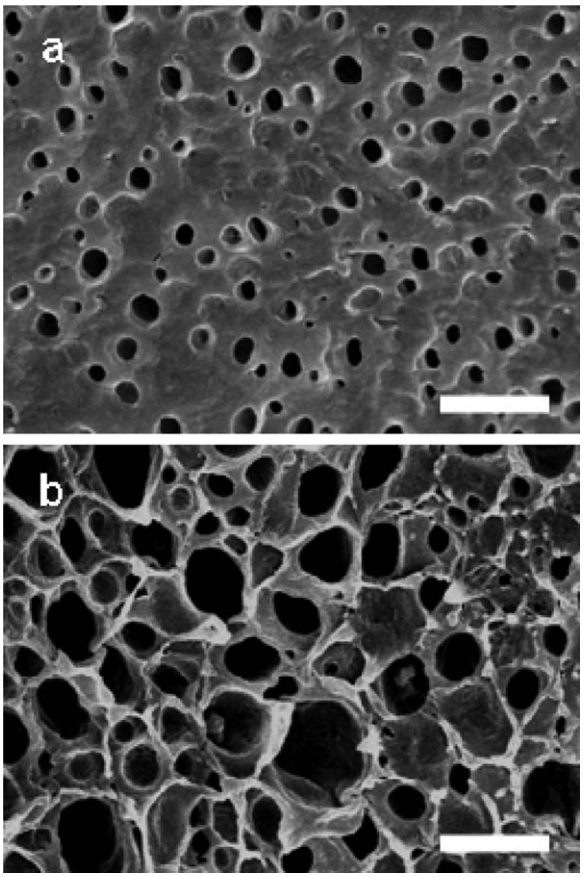

Figure 1. SEM micrographs revealing phase morphology of PVDF/PA6 blends with (a) 15 wt % and (b) 30 wt % PA6 content, respectively. The PA6 droplets were removed by formic acid treatment, and the scale bars correspond to 1 μm.

comparison, neat PVDF and PA6 were also subjected to same procedures. Samples for mechanical stretching and structural characterizations were prepared by hot pressing at 240 °C and cooling down to room temperature in a cold press.

Characterizations

Thermal behaviors were recorded by a TA Q2000 differential scanning calorimetry (DSC) under a flowing nitrogen atmosphere at a rate of 10 °C/min. Samples were melted at 240 °C for 5 min and then cooled down to 40 °C to record crystallization traces. Thereafter, melting traces were obtained by reheating up to 240 °C. Rheological measurements were conducted by a TA discovery hybrid rheometer (DHR-2) with a 25 mm parallel-plate geometry having a gap of 0.9 mm under a flowing nitrogen atmosphere. Dynamic oscillatory shear measurements were carried out at 240 °C in the frequency range between 0.01 and 10 Hz with a strain of 1%. The chosen strain was well located in the linear viscoelastic regime, as determined by a strain sweep prior to each measurement. Mechanical stretching was conducted by a universal testing machine at a cross-head speed of 5 mm/min at room temperature. Engineering stress–strain curves were deduced from measured force and displacement. Fourier-transform infrared spectroscopy (FTIR) measurements were performed by a Thermo Nicolet FTIR spectrometer with a resolution of 4 cm^{-1} at room temperature. A polarizer was used to obtain spectra parallel and perpendicular to stretching direction for mechanically stretched samples. Allowing for neck formation during stretching, true strain instead of engineering strain was adopted by measuring separation of inkmarks preprinted on the samples. X-ray diffraction (XRD) measurements were conducted by a Bruker D8 ADVANCE X-ray diffractometer at room temperature; and the wavelength of the X-ray was 0.154 nm. Morphology was disclosed by a Nova NanoSEM 450 scanning electron microscope (SEM) at room temperature. Samples for SEM observation were prepared by cryofracture in liquid nitrogen.

RESULTS AND DISCUSSION

Figure 1 shows the SEM micrographs of PVDF/PA6 blends after removal of PA6 component by formic acid. Submicron PA6 droplets are dispersed in the PVDF matrix, as a result of specific interactions between the polar amide group in PA6 and the CF_2 groups in PVDF.[17,18] The PA6 droplets become large with its content in the blends due to enhanced coalescence during mixing. Thus, it can be roughly deduced that the interparticle distance is decreased with the increasing of PA6 content in the blends. It

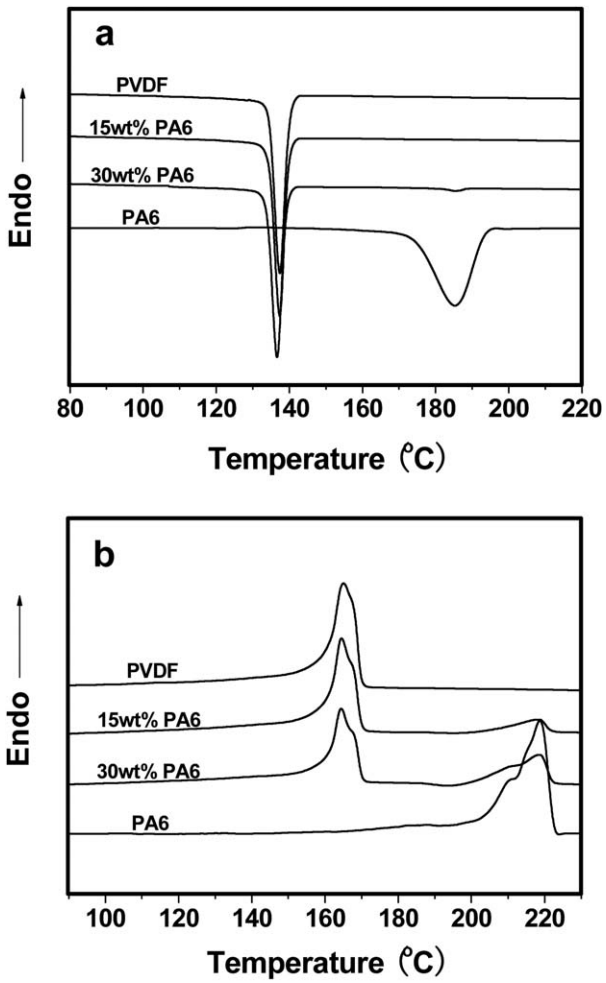

Figure 2. (a) DSC cooling and (b) heating traces of PVDF/PA6 with the indicated PA6 content, respectively. For comparison, those of neat PVDF and PA6 were included.

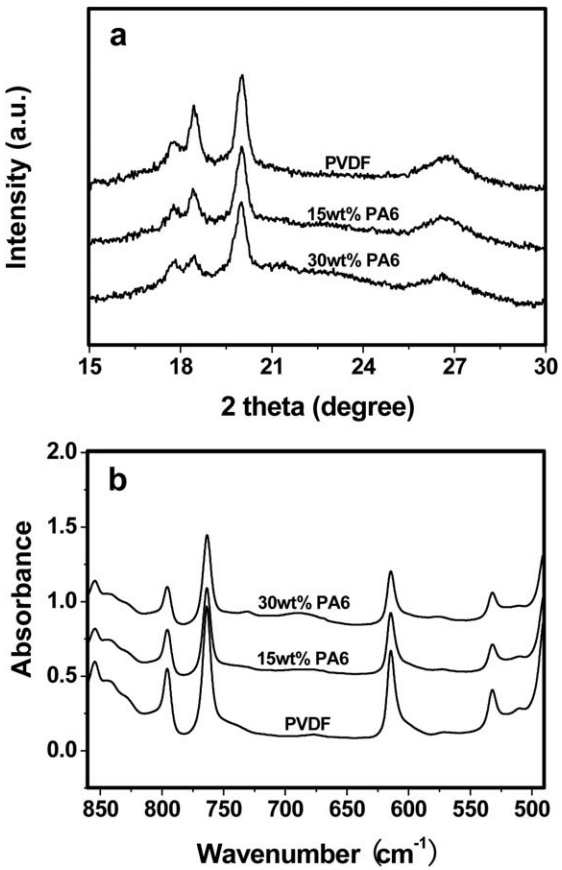

Figure 3. (a) XRD profile and (b) FTIR spectra of PVDF and its blends with the indicated PA6 content, respectively.

means available space for PVDF matrix is reduced at high PA6 content, which could affect molecular mobility in the melt.

Submicron PA6 droplets have little influence on crystallization and melting behaviors of PVDF matrix, as depicted by DSC traces in Figure 2. PVDF matrix has a crystallization temperature around 137 °C, irrespective of PA6 content. It is nearly same to that of neat PVDF. Meanwhile, melting of PVDF crystals, with an endothermic peak around 165 °C, is almost identical for neat PVDF and its blends with PA6. The crystallization behaviors in the immiscible PVDF/PA6 blends are totally different from that observed in the miscible blends, where crystallization and melting of PVDF component are significantly suppressed.[23–25] On the other hand, crystallization in the submicron PA6 droplets is retarded to a large extent. Only a small exothermic peak around 185°C is observed in the blends with 30 wt % PA6. It is correlated with the suppressed nucleation and growth of crystals in the submicron droplets, i.e., confined crystallization.[6,26] Therefore, most crystallization in the submicron PA6 droplets can only occur upon heating, responsible for the appearance of an exothermic peak around 195°C before dominant melting of PA6 crystals.

The crystal form of PVDF matrix also remains intact, irrespective of PA6 content in the blends. It is illustrated by XRD profiles and FTIR spectra in Figure 3. Only the α-form is exhibited by the PVDF matrix, same to that observed in neat PVDF. The α-form has characteristic reflections at 2θ around 18.4, 20, and 26.6° in the XRD profiles, and typical absorption at 764, 796 cm^{-1} in the FTIR spectra.[27,28] In combination with above DSC results, it suggests that crystallization habits of PVDF matrix from melt are little affected in the presence of immiscible PA6 droplets.

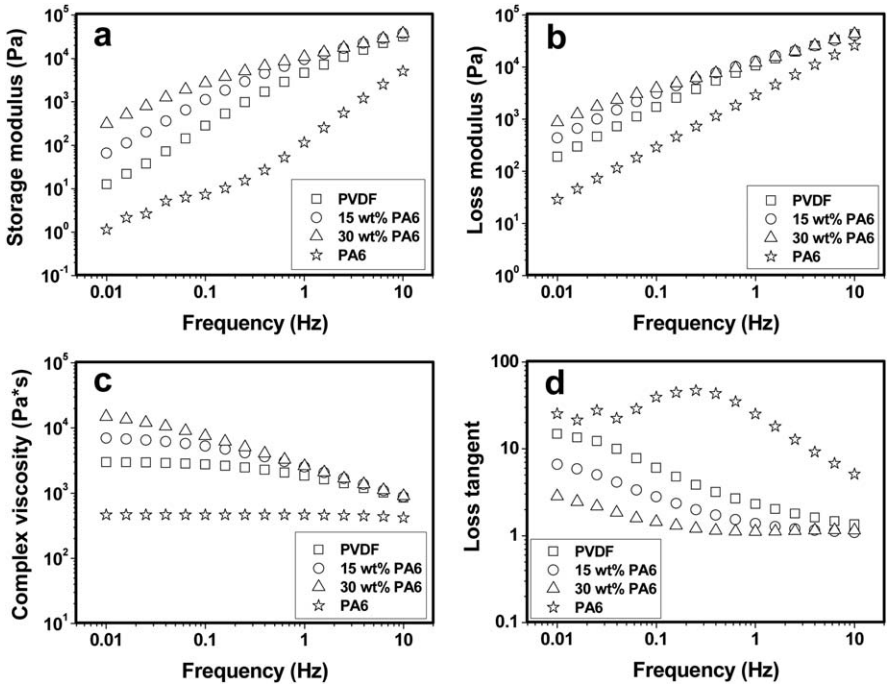

Figure 4. Rheological properties of PVDF/PA6 blends with the indicated PA6 content at 240 °C: (a) storage modulus, (b) loss modulus, (c) complex viscosity, and (d) loss tangent. For comparison, those of neat PVDF and PA6 were included.

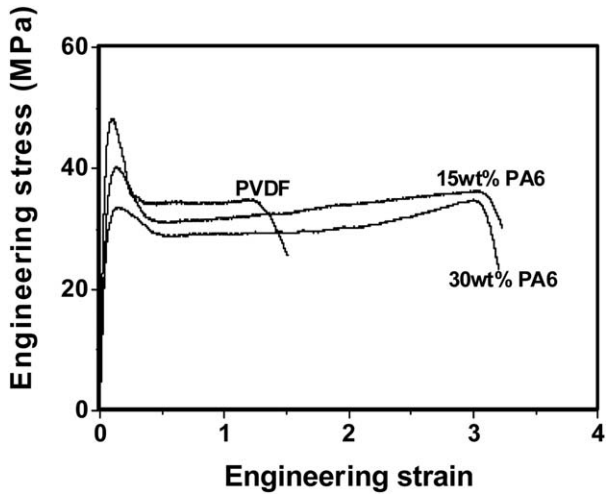

Figure 5. Engineering stress–strain curves of PVDF and its blends with the indicated PA6 content.

Figure 4 gives the linear viscoelastic behaviors of PVDF/PA6 blends as a function of frequency. For comparison, those of neat PVDF and PA6 are included. Neat PA6 has lower melt elasticity (storage modulus) and complex viscosity than neat PVDF in the measured frequency range. However, the presence of PA6 droplets in the PVDF matrix significantly enhances melt elasticity and complex viscosity at low frequencies. The enhancement effect is increased with PA6 content in the blends. At high frequencies, the enhancement effect disappears, and the curves of storage modulus and complex viscosity in the blends merge with those of neat PVDF. That is, viscoelastic responses in the blends at high frequencies are dominated by PVDF matrix rather than by PA6 droplets. On the other hand, loss tangent reflecting relaxation process is reduced in the blends, as compared to that of neat PVDF. It suggests that submicron PA6 droplets suppress molecular relaxation of PVDF matrix in the melt to some extent.

The enhanced elasticity and suppressed relaxation in the PVDF/PA6 blends should arise from submicron dispersion of PA6 droplets in the PVDF matrix. That is, chain motion in the PVDF matrix is significantly restrained by large available phase interfaces,[11] albeit of low melt elasticity and viscosity of PA6 droplets themselves. It is intensified by the increase in the interfacial area and the decrease in the interparticle distance at high PA6 content such as 30 wt %. The change in viscoelastic properties in the PVDF/PA6 blends is much outstanding, as compared to other immiscible PVDF blends with coarse phase morphology. For instance, in a study regarding PVDF blends with polylactide (PLA), micron PLA droplets only have a slight effect on the viscoelastic properties of the blends.[29]

Figure 5 shows the engineering stress–strain curves of neat PVDF and the blends with the indicated PA6 content. The presence of submicron PA6 droplets reduces yield stress of the blends because of stress concentrating effect. It becomes significant with the increasing of PA6 content in the blends. The decrease in yield stress results in easy deformation and thus high elongation at break of the blends, as compared to neat PVDF. Furthermore, significant plastic deformation of PVDF matrix is facilitated by simultaneous elongation of dispersed PA6 droplets upon stretching. As an example, Figure 6 shows the SEM micrographs of PVDF/PA6 blends with 15 wt % PA6 content after being stretched up to fracture. Good interfacial adhesion between two components prevents debonding at interfaces, as demonstrated by morphological observation on the stretched samples without formic acid treatments. As a comparison, numerous elongated voids along stretching direction, corresponding to elongated PA6 droplets, appear on the stretched samples after formic acid treatments. Thus, cooperative deformation of PA6 droplets, with little interfacial debonding, is responsible for remarkable elongation of the blends.

It is well established that the α-form in PVDF can be converted into the β-form under mechanical stretching.[30–32] As illustrated above, the α-form prevails in the PVDF matrix, irrespective of PA6 content. Thus, it is of great interest to explore α→β crystal transformation in the PVDF/PA6 blends induced by stretching. As it is very powerful to distinguish crystal forms of PVDF, FTIR technique was used to disclose crystal transformation with respect to strains.[27,28] Figure 7 presents polarized FTIR spectra of the blends parallel and perpendicular to stretching direction, respectively. Of note, due to inhomogenous deformation (i.e., necking) during stretching, true strain rather than engineering strain was adopted. Mechanical stretching results in the

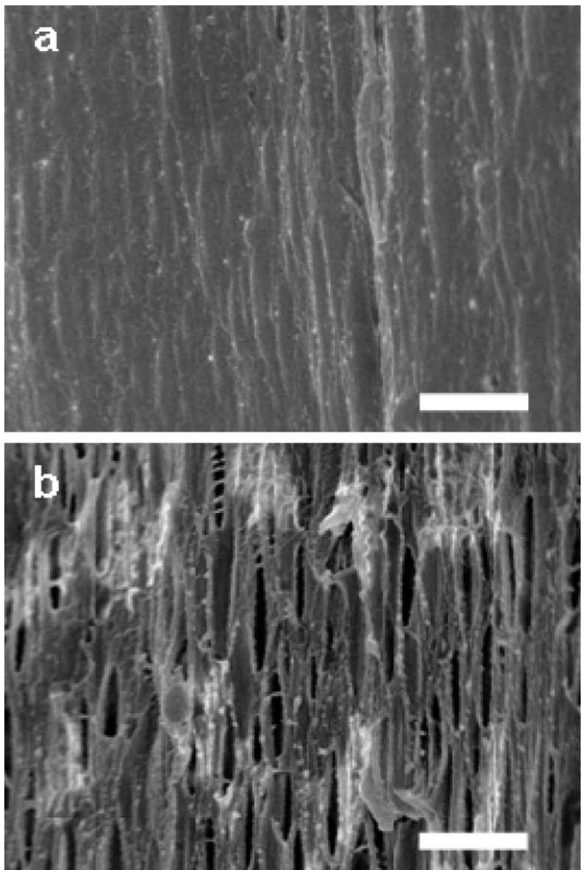

Figure 6. SEM micrographs of cross-sections of PVDF/PA6 blends with 15 wt % PA6 content after being stretched up to fracture: (a) as-fractured, (b) removal of PA6 droplets by formic acid. The scale bars correspond to 1 μm, and the stretching direction was nearly vertical.

formation of the β-form as demonstrated by the appearance of the absorptions at 840 and 510 cm^{-1}.[27,28,31] It becomes significant at large strains accompanied by gradual weakening of the absorptions at 796 and 764 cm^{-1} that are contributed by the α-form.

To get detailed information about $\alpha \rightarrow \beta$ crystal transformation, relative fraction of the β-form, $F(\beta)$, was calculated according to eqs. (1) and (2).

$$A=(A_{//}+2A_{\perp})/3 \quad (1)$$

$$F(\beta)=A_{510}/(A_{510}+A_{764}) \quad (2)$$

where $A_{//}$ and $A_{\perp}$ is the absorbance of the desired IR band parallel and perpendicular to the stretching direction, respectively.

Figure 8 shows the corresponding results for the blends with the indicated PA6 content. Note that, due to severe necking and premature fracture, only FTIR result at a true strain of 3 was obtained for neat PVDF. As expected, relative fraction of the β-form is increased with true strains as a result of gradual crystal transformation upon stretching. It is independent of PA6 content in the blends. However, the presence of submicron PA6 droplets

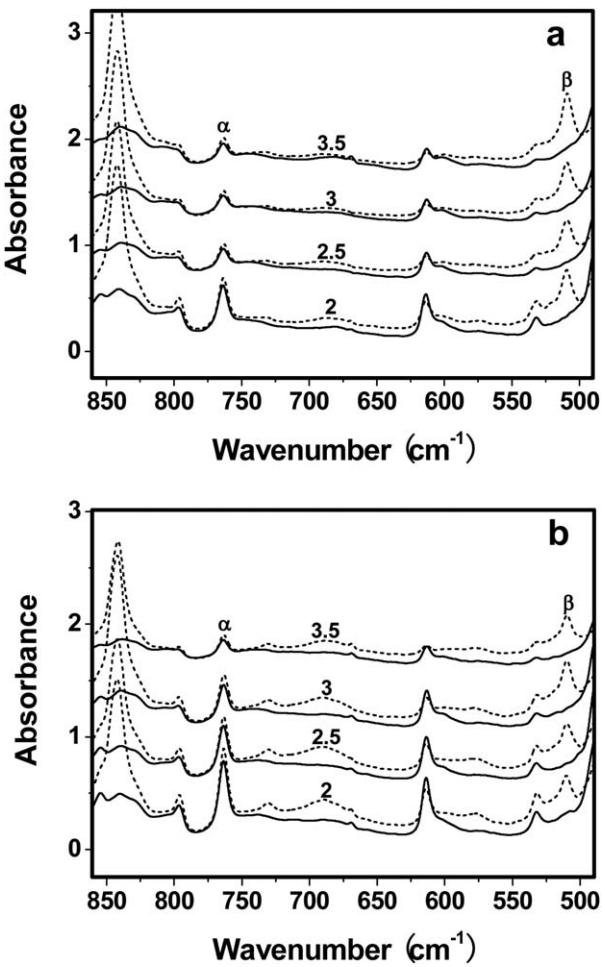

Figure 7. Polarized FTIR spectra of PVDF/PA6 blends with (a) 15 wt % and (b) 30 wt % PA6 content after being stretched to the indicated true strain. The solid and dashed lines represent spectra parallel and perpendicular to the stretching direction, respectively.

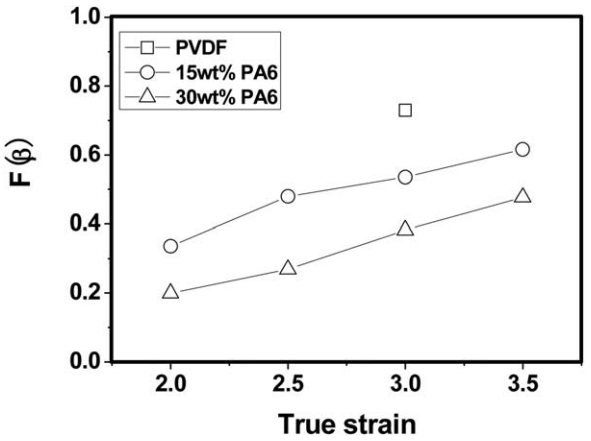

Figure 8. Relative fraction of the β-form in the PVDF/PA6 blends with the indicated PA6 content after being stretched to various true strains. The data of neat PVDF stretched to a true strain of 3 was included.

significantly suppresses mechanical crystal transformation in the PVDF matrix, as compared to that observed in the neat PVDF. Moreover, the suppressed effect becomes more severe in the blends with higher PA6 content. It is well established that $\alpha \rightarrow \beta$ crystal transformation is mainly dominated by the exerted stress during stretching. Thus, the suppressed crystal transformation in the blends could be correlated with low stress transferred to the α-form of PVDF matrix (Figure 5).

CONCLUSIONS

This study gives comprehensive insights into rheological properties and mechanical crystal transformation in the PVDF/PA6 blends. Due to submicron droplet morphology and specific interactions, melt elasticity and viscosity of the blends are significantly enhanced. However, the presence of submicron PA6 droplets suppresses $\alpha \rightarrow \beta$ crystal transformation in the PVDF matrix to a large extent, which could be related to the stress decrement during mechanical stretching. The findings demonstrate that, although other properties are improved, blending PVDF with PA6 is not favorable for the generation of the β-form upon mechanical stretching.

ACKNOWLEDGMENTS

This work is financially supported by the National Natural Science Foundation of China (No. 51163001).

REFERENCES

1. Li, Y.; Oono, Y.; Kadowaki, Y.; Inoue, T.; Nakayama, K.; Shimizu, H. *Macromolecules* **2006**, *39*, 4195.
2. Xu, C.; Wang, Y.; Chen, Y. *Polym. Test.* **2014**, *33*, 179.
3. Shimizu, H.; Li, Y.; Kaito, A.; Sano, H. *Macromolecules* **2005**, *38*, 7880.
4. Li, Y.; Iwakura, Y.; Zhao, L.; Shimizu, H. *Macromolecules* **2008**, *41*, 3120.
5. Yin, M.; Zhu, Y.; Lv, R.; Na, B.; Liu, Q. *RSC Adv.* **2014**, *4*, 39491.

6. Zhong, G.; Su, R.; Zhang, L.; Wang, K.; Li, Z.; Fong, H.; Zhu, L. *Polymer* **2012**, *53*, 4472.
7. Dhevi, D. M.; Prabu, A. A.; Pathak, M. *Polymer* **2014**, *55*, 886.
8. Yoon, L. K.; Kyu, B. *J. Appl. Polym. Sci.* **2000**, *78*, 1374.
9. Kaito, A.; Iwakura, Y.; Li, Y.; Shimizu, H. *J. Polym. Sci. Polym. Phys.* **2008**, *46*, 1376.
10. Kim, K. J.; Cho, H. W.; Yoon, K. J. *Eur. Polym. J.* **2003**, *39*, 1249.
11. Ma, H.; Yang, Y. *Polym. Test.* **2008**, *27*, 441.
12. Mascia, L.; Hashim, K. *Polymer* **1998**, *39*, 369.
13. Moussaif, N.; Jérôme, R. *Polymer* **1999**, *40*, 3919.
14. Yang, J.; Feng, C.; Dai, J.; Zhang, N.; Huang, T.; Wang, Y. *Polym. Int.* **2013**, *62*, 1085.
15. Dong, W.; Wang, H.; He, M.; Ren, F.; Wu, T.; Zheng, Q.; Li, Y. *Ind. Eng. Chem. Res.* **2015**, *54*, 2081.
16. Na, B.; Xu, W.; Lv, R.; Li, Z.; Tian, N.; Zou, S. *Macromolecules* **2010**, *43*, 3911.
17. Liu, Z. H.; Marechal, P.; Jérôme, R. *Polymer* **1998**, *39*, 1779.
18. Kaito, A.; Iwakura, Y.; Li, Y.; Nakayama, K.; Shimizu, H. *Macromol. Chem. Phys.* **2007**, *208*, 504.
19. Vo, L. T.; Giannelis, E. P. *Macromolecules* **2007**, *40*, 8271.
20. Martins, P.; Lopes, A. C.; Lanceros-Mendez, S. *Prog. Polym. Sci.* **2014**, *39*, 683.
21. Vijayakumar, R. P.; Khakhar, D. V.; Misra, A. *J. Appl. Polym. Sci.* **2010**, *117*, 3491.
22. Sajkiewicz, P.; Wasiak, A.; Goclowski, Z. *Eur. Polym. J.* **1999**, *35*, 423.
23. Li, M.; Stingelin, N.; Michels, J. J.; Spijkman, M. J.; Asadi, K.; Feldman, K.; Blom, P. W. M.; de Leeuw, D. M. *Macromolecules* **2012**, *45*, 7477.
24. Okabe, Y.; Murakami, H.; Osaka, N.; Saito, H.; Inoue, T. *Polymer* **2010**, *51*, 1494.
25. Qiu, Z.; Yan, C.; Lu, J.; Yang, W.; Ikehara, T.; Nishi, T. *J. Phys. Chem. B* **2007**, *111*, 2783.
26. Tol, R. T.; Mathot, V. B. F.; Groeninckx, G. *Polymer* **2005**, *46*, 369.
27. Zhu, Y.; Li, C.; Na, B.; Lv, R.; Chen, B.; Zhu, J. *Mater. Chem. Phys.* **2014**, *144*, 194.
28. Zheng, J.; He, A.; Li, J.; Han, C. C. *Macromol. Rapid Commun.* **2007**, *28*, 2159.
29. Xie, Q.; Ke, K.; Jiang, W. R.; Yang, W.; Liu, Z. Y.; Xie, B. H.; Yang, M. B. *J. Appl. Polym. Sci.* **2013**, *129*, 1686.
30. Maier, G. A.; Wallner, G.; Lang, R. W.; Fratzl, P. *Macromolecules* **2005**, *38*, 6099.
31. Salimi, A.; Yousefi, A. A. *Polym. Test.* **2003**, *22*, 699.
32. Li, L.; Zhang, M.; Rong, M.; Ruan, W. *RSC Adv.* **2014**, *4*, 3938.